

# Computing the Topological Entropy of Braids, Fast

Matthew D. Finn and Jean-Luc Thiffeault

Department of Mathematics  
Imperial College London

Lorentz Centre, 18 May 2006

# Surface Diffeomorphisms

- We consider a family of smooth diffeos  $f_t : M \rightarrow M$ , parametrised by  $t \in [0, 1]$ .
- $f_1$  leaves invariant  $n$  **punctures** in the surface  $M$ .
- The motion of the punctures traces a **braid**.
- This braid implies a minimum topological entropy for  $f_1$ .
- Given only the abstract braid, in terms of group generators, how do we compute its topological entropy?
- We want to do this for very large braids, so we need a method that is computationally efficient.

# Topological Entropy

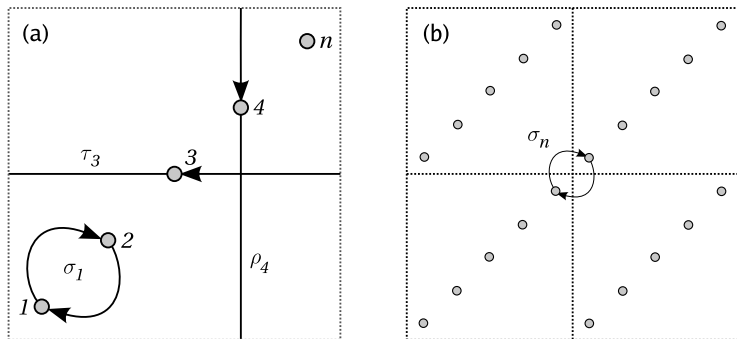
- Can compute the topological entropy in several ways:
  - Train-tracks algorithm such as Bestvina–Handel (1995).
  - (Poor) lower bound using Burau representation (Kolev 1989).
- Implementation of B–H algorithm due to Toby Hall takes Artin braid group generators as input.
- Prohibitive for even a small ( $\sim 40$ ) number of generators.
- No simple implementation for the torus.

# The Algorithm of Moussafir

- Recently, Moussafir (2006) introduced a fast method that converges to the exact entropy of a braid.
- Uses Dynnikov coordinates (2002) to encode the number of crossings between a lamination and a reference line.
- Less information than train tracks, but at lower cost.
- Here: derive such an algorithm for braids on the torus.
- Allows a topological analysis of bi-periodic systems, such as the sine flow.

## Braid Group Generators

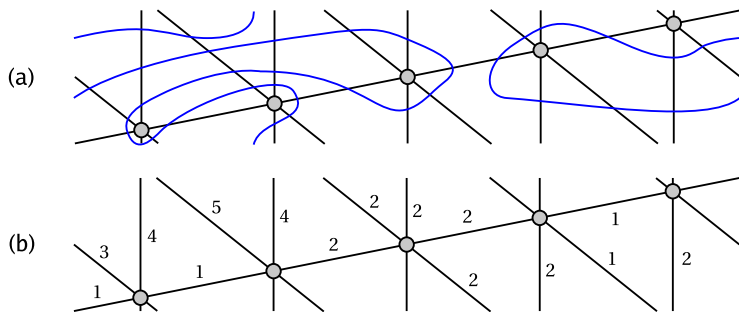
Birman (1969) defines three types of generators for the braid group on the torus.



The usual Artin braid group is a subgroup that only uses  $\sigma$ .

## Lamination and Triangulation

A lamination is an equivalence class of simple closed curves.

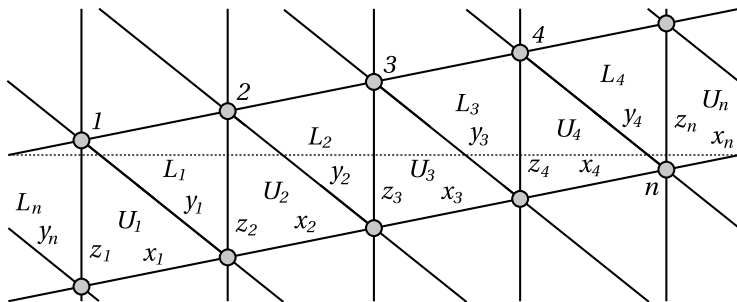


The triangulation links the punctures, but is not unique. We count the crossings between the lamination and triangulation.

The triangulation is static, but the lamination is evolved under the diffeomorphism.

## Triangulation (2)

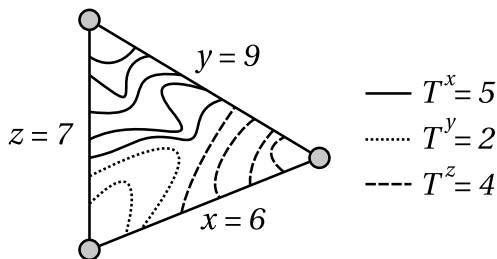
We often show multiple copies of the domain (universal cover). A dotted line separates copies.



$U$  and  $L$  label triangles,  $x, y, z$  are crossing numbers.

## Edge-linking Numbers

Any part of the lamination passing between edges  $x$  and  $y$  is counted by  $T^z$ , similarly for  $T^x$  and  $T^y$ .



$$T^x = \frac{1}{2}(y + z - x)$$

$$T^y = \frac{1}{2}(x + z - y)$$

$$T^z = \frac{1}{2}(x + y - z)$$

The lamination is always assumed to be 'pulled tight.'

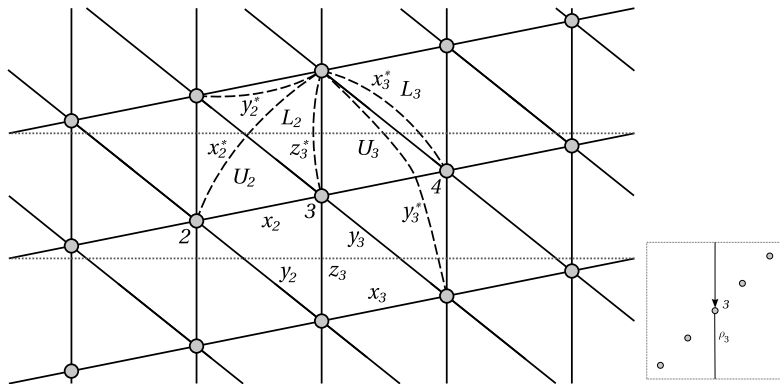


## Crossing Update Rules

- The diffeomorphism changes the lamination as described using braid group generators for the punctures.
- The crossing numbers with the triangulation also change.
- The goal is to calculate the 'update rules' for the crossing numbers, given the generators.
- The preimage of edge  $e$  is  $e^*$ , which is a curve that becomes  $e$  after the braid operation.
- The number of crossings of  $e^*$  before the braid operation has to be equal to the number of crossings with  $e$ .
- But  $e^*$  is usually not part of the triangulation!
- Like playing Minesweeper: we know some numbers, we must deduce others.

## Crossing Update Rules for $\rho_3$

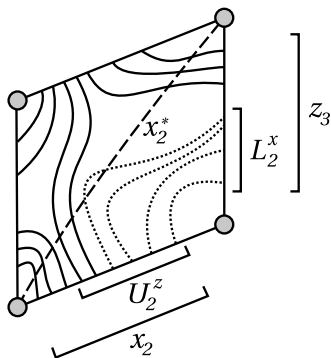
Only edges  $x_2$ ,  $y_2$ ,  $x_3$ ,  $y_3$  and  $z_3$  change.



$x_2$  and  $y_3$  are the preimages of  $y_2$  and  $x_3$ , respectively, so  $y_2^* = x_2$  and  $x_3^* = y_3$ . The edge  $z_3$  is its own preimage,  $z_3^* = z_3$ .

## The Quadrilateral Puzzle

The preimages of  $x_2$  and  $y_3$  are not edges in the triangulation. We must deduce their crossing numbers.



Curves entering  $x_2$  and  $z_3$  must cross  $x_2^*$ , unless they loop directly from  $x_2$  to  $z_3$ . The number of these loops is exactly  $\min(U_2^z, L_2^x)$ . Hence the number of preimage crossings is  $x_2 + z_3 - 2 \min(U_2^z, L_2^x)$ .

## Crossing Update Rules for $\rho_i$

For general  $i$ , we have

$$x_{i-1}^* = x_{i-1} + z_i - 2 \min(U_{i-1}^z, L_{i-1}^x)$$

$$y_{i-1}^* = x_{i-1}$$

$$x_i^* = y_i$$

$$y_i^* = z_i + y_i - 2 \min(U_i^y, L_i^z)$$

$$z_i^* = z_i$$

## Crossing Update Rules for $\rho_i^{-1}$

Because of the  $\pi$ -rotational symmetry of the triangulation, we easily find the update rules for  $\rho_i^{-1}$  directly from that for  $\rho_i$ :

$$x_{i-1}^* = y_{i-1}$$

$$y_{i-1}^* = y_{i-1} + z_i - 2 \min(U_{i-1}^z, L_{i-1}^y)$$

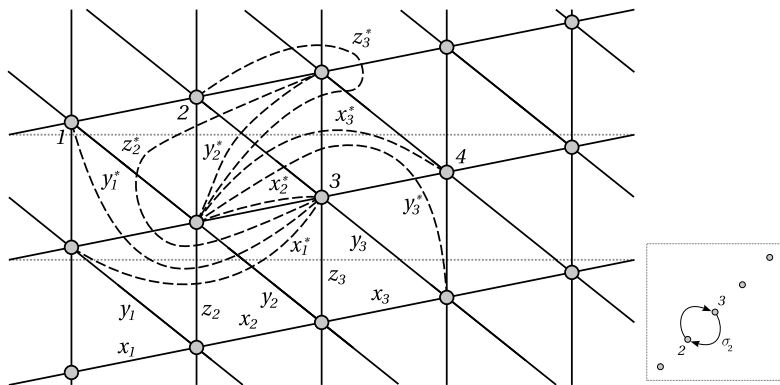
$$x_i^* = z_i + x_i - 2 \min(U_i^x, L_i^z)$$

$$y_i^* = x_i$$

$$z_i^* = z_i$$

## Crossing Update Rules for $\sigma_2$

Two punctures are permuted clockwise! Many more edges involved.

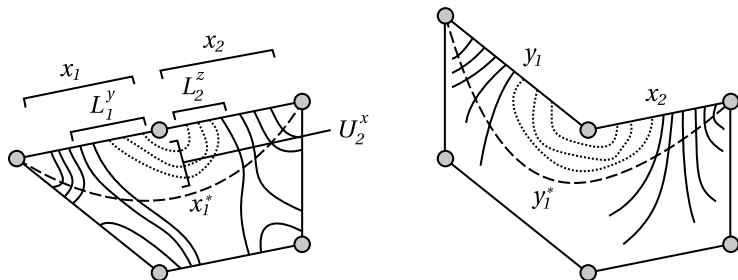


Edge  $x_2$  is its own preimage, but all other preimages require some Minesweeping. Edge  $y_2^*$  is of the quadrilateral form.

## Crossing Puzzle for $x_1^*$ and $y_1^*$

The number of crossings with preimage  $x_1^*$  is given by the number of curves crossing  $x_1$  and  $x_2$ , minus twice the number of loops directly between  $x_1$  and  $x_2$ , given by  $\min(L_1^y, U_2^x, L_2^z)$ . Hence  $x_1^* = x_1 + x_2 - 2 \min(L_1^y, U_2^x, L_2^z)$ .

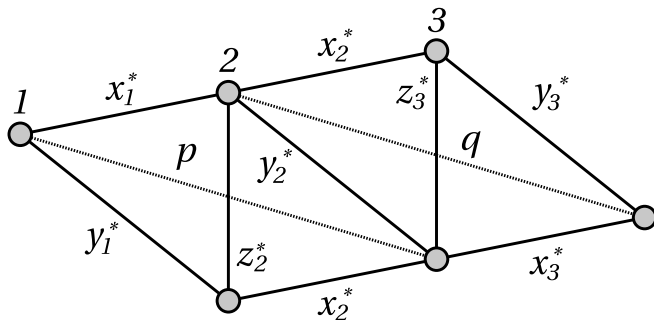
The preimage problem for  $y_1^*$  is similar, but involves 4 triangles, so that  $y_1^* = y_1 + x_2 - 2 \min(U_1^z, L_1^y, U_2^x, L_2^z)$ .



Preimages  $x_3^*$  and  $y_3^*$  are handled in the same way.

## Crossing Puzzle for $z_2^*$ and $z_3^*$

Still need to find  $z_2^*$  and  $z_3^*$ , which pass through 7 (!) triangles. We deduce  $z_2^*$  and  $z_3^*$  by invoking the quadrilateral solution with the *updated* crossing numbers. We introduce temporary edges  $p$  and  $q$  directly between punctures 1 and 3 and between 2 and 4.



The preimage of  $p$  is  $y_1$ , and the preimage of  $q$  is  $y_3$ . Since  $x_1^*$ ,  $y_1^*$ ,  $p$ ,  $x_2^*$ ,  $y_2^*$ ,  $q$ ,  $x_3^*$  and  $y_3^*$  are known,  $z_2^*$  and  $z_3^*$  follow.



## Crossing Update Rules for $\sigma_i$

Putting it all together,

$$x_{i-1}^* = x_{i-1} + x_i - 2 \min(L_{i-1}^y, U_i^x, L_i^z)$$

$$y_{i-1}^* = y_{i-1} + x_i - 2 \min(U_{i-1}^z, L_{i-1}^y, U_i^x, L_i^z)$$

$$x_i^* = x_i$$

$$y_i^* = z_i + x_i - 2 \min(U_i^x, L_i^z)$$

$$z_i^* = x_{i-1}^* + y_{i-1}^* - \min(y_{i-1}^* + y_{i-1} - x_i^*, x_{i-1}^* + y_{i-1} - y_i^*)$$

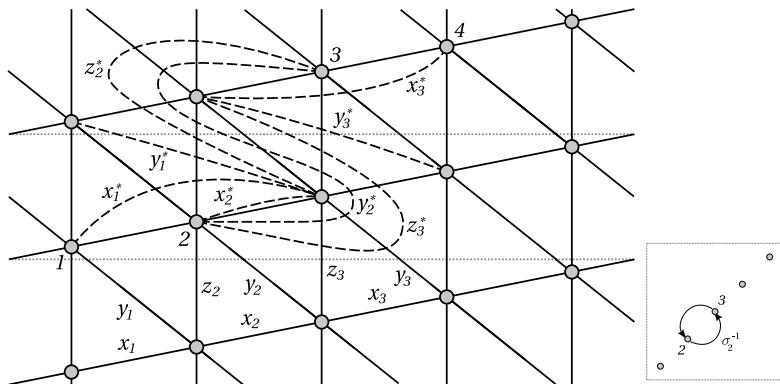
$$x_{i+1}^* = x_i + x_{i+1} - 2 \min(U_i^z, L_i^x, U_{i+1}^y)$$

$$y_{i+1}^* = x_i + y_{i+1} - 2 \min(U_i^z, L_i^x, U_{i+1}^y, L_{i+1}^z)$$

$$z_{i+1}^* = x_i^* + y_i^* - \min(x_i^* + y_{i+1} - y_{i+1}^*, y_i^* + y_{i+1} - x_{i+1}^*).$$

## Crossing Update Rules for $\sigma_i^{-1}$

Lack of reflection symmetry about a vertical line through the midpoint of two punctures means that it is not possible to deduce the update rules for  $\sigma_i^{-1}$  by a relabelling in the rules for  $\sigma_i$ .



The preimage curve  $y_i^*$  is the most complicated yet, as it passes through ten triangles.

## Crossing Update Rules for $\sigma_i^{-1}$ (2)

However, things proceed pretty much as before, so we quote the result:

$$x_{i-1}^* = x_{i-1} + x_i - 2 \min(U_{i-1}^z, L_{i-1}^x, U_i^y)$$

$$y_{i-1}^* = y_{i-1} + x_i - 2 \min(L_{i-1}^x, U_i^y)$$

$$x_i^* = x_i$$

$$y_i^* = x_i^* + z_i^* - \min(z_i^* + y_i - x_i^*, x_i^* + y_i - z_{i+1}^*)$$

$$z_i^* = x_i + y_i - 2 \min(U_i^x, L_{i-1}^y, U_{i-1}^z, L_{i-1}^x, U_i^y)$$

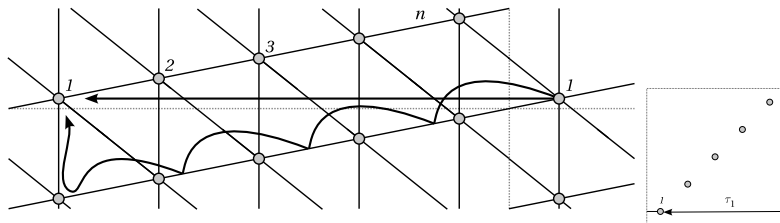
$$x_{i+1}^* = x_i + x_{i+1} - 2 \min(L_i^y, U_{i+1}^x, L_{i+1}^z)$$

$$y_{i+1}^* = y_i + x_{i+1} - 2 \min(L_i^x, U_{i+1}^y) = x_i + y_{i+1} - 2 \min(L_i^y, U_{i+1}^x)$$

$$z_{i+1}^* = x_i + y_i - 2 \min(L_i^y, U_{i+1}^x, L_{i+1}^z, U_{i+1}^y, L_i^x)$$

## Crossing Update Rules for $\tau_1$

Our choice of triangulation makes  $\rho_i$  easy but  $\tau_i$  quite complicated. Instead of attacking this problem directly,  $\tau_1$  can be achieved by a sequence of  $\sigma_i$ , including  $\sigma_n$ , followed by one  $\rho_1^{-1}$ .



The same technique works for  $\tau_i^{-1}$ .

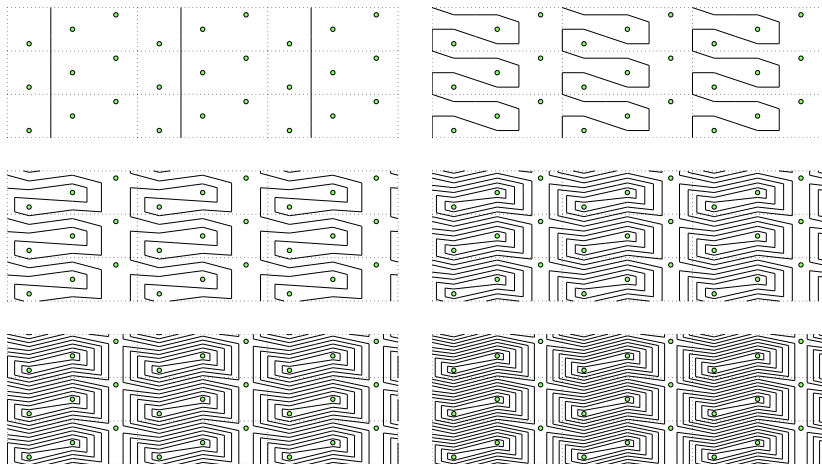
## Crossing Update Rules for $\tau_i$

To calculate the updated set of crossing numbers  $\{x_i, y_i, z_i\}$  for  $\tau_i$  do the following:

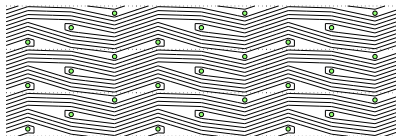
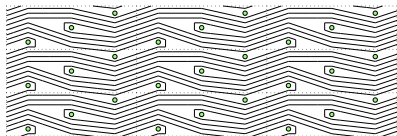
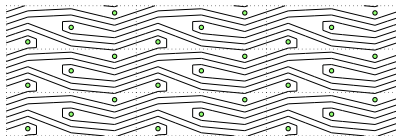
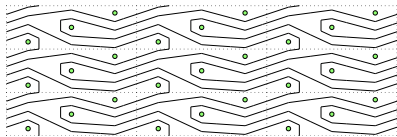
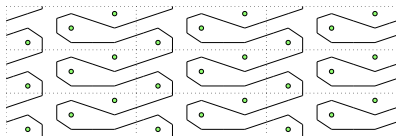
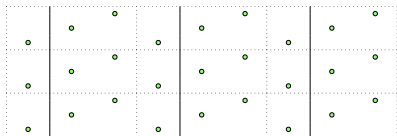
1. Perform, in turn,  $\sigma_{i-1}^{-1}, \sigma_{i-2}^{-1}, \dots, \sigma_{i+2}^{-1}$  and  $\sigma_{i+1}^{-1}$ . Treat the indices 'modulo'  $n$ , so that  $\sigma_n^{-1}$  follows  $\sigma_1^{-1}$ .
2. Relabel  $x_i \leftarrow x_{i+1}, y_i \leftarrow y_{i+1}$  and  $z_i \leftarrow z_{i+1}$ . This leaves all punctures except the  $i$ th one in the correct position.
3. Perform  $\rho_i^{-1}$ .

## A Finite-Order Braid: $\sigma_1$

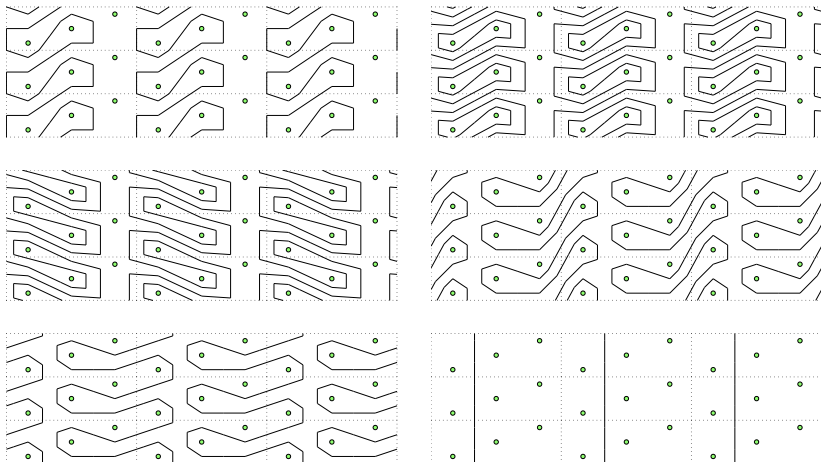
We can reconstruct a lamination from the crossing numbers, so our update rules allow us to draw it 'on the fly.'



# Another Finite-Order Braid: $\tau_2$



# The Identity Braid $\sigma_1^{-2}\rho_1^{-1}\tau_2\rho_1\tau_2^{-1}$





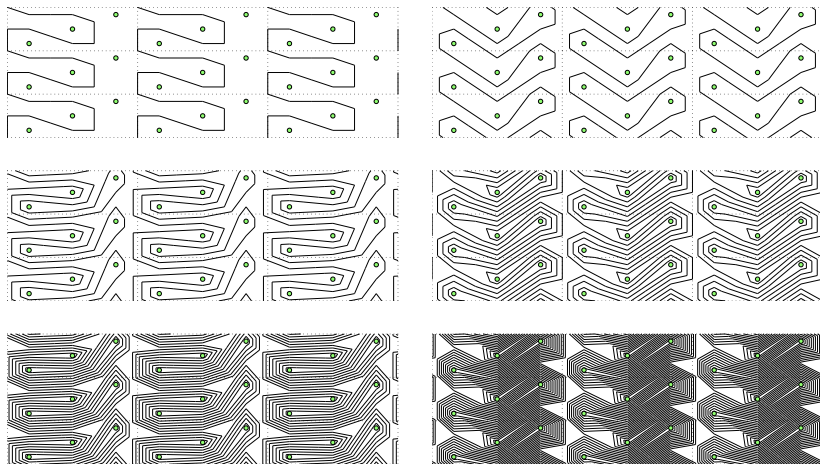
## Calculating Topological Entropy

For braids on the sphere, Moussafir (2006) showed that the number of crossings grows at the same rate as the topological entropy implied by the braid. The same result applies here:

$$\lambda^\dagger = \log \sum_i (x_i^* + y_i^* + z_i^*) - \log \sum_i (x_i + y_i + z_i)$$

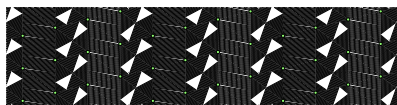
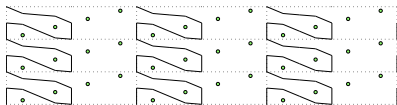
as the number of crossings goes to infinity.

# The Golden Braid: $\sigma_1\sigma_2^{-1}$



Topological entropy is  $2 \log \left( \frac{1}{2}(1 + \sqrt{5}) \right)$ .

# The Silver Braid: $\sigma_1\sigma_3\sigma_2^{-1}\sigma_4^{-1}$



Topological entropy is  $4 \log(1 + \sqrt{2})$ .

## Convergence to the Topological Entropy

Convergence of  $\lambda^\dagger$  to the exact braid entropy  $\lambda$  appears to be exponential (provided the braid has a pseudo-Anosov component).

| iteration | total crossings  | entropy $\lambda^\dagger$ | error $ \lambda - \lambda^\dagger $ |
|-----------|------------------|---------------------------|-------------------------------------|
| 1         | 24               | 2.48490664978800          | 0.72215947574891                    |
| 2         | 154              | 1.85889877206568          | 0.09615159802660                    |
| 3         | 912              | 1.77868738766070          | 0.01594021362162                    |
| 4         | 5330             | 1.76546652708556          | 0.00271935304647                    |
| 5         | 31080            | 1.76321328732169          | 0.00046611328261                    |
| 6         | 181162           | 1.76282713309230          | 0.00007995905321                    |
| 7         | 1055904          | 1.76276089245107          | 0.00001371841199                    |
| 8         | 6154274          | 1.76274952773491          | 0.00000235369583                    |
| 9         | 35869752         | 1.76274757786911          | 0.00000040383002                    |
| 10        | 209064250        | 1.76274724332535          | 0.00000006928627                    |
| 11        | 1218515760       | 1.76274718592673          | 0.00000001188765                    |
| 12        | 7102030322       | 1.76274717607868          | 0.00000000203960                    |
| 13        | 41393666184      | 1.76274717438903          | 0.00000000034994                    |
| 14        | 241259966794     | 1.76274717409913          | 0.00000000006004                    |
| 15        | 1406166134592    | 1.76274717404939          | 0.00000000001030                    |
| 16        | 8195736840770    | 1.76274717404085          | 0.00000000000177                    |
| 17        | 47768254910040   | 1.76274717403939          | 0.00000000000030                    |
| 18        | 278413792619482  | 1.76274717403914          | 0.00000000000005                    |
| 19        | 1622714500806864 | 1.76274717403910          | 0.00000000000001                    |
| 20        | 9457873212221714 | 1.76274717403908          | 0.00000000000000                    |

## The Sine Flow

Area-preserving map obtained by integrating alternating sine flow, defined over  $0 \leq x, y < 1$ , period  $T$ .

$$x_{n+\frac{1}{2}} = x_n + \frac{1}{2} T \sin(2\pi y_n)$$

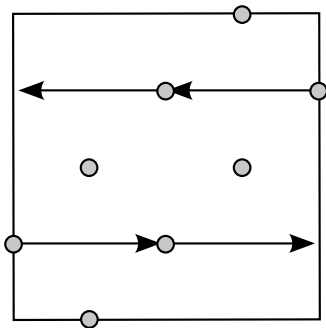
$$y_{n+\frac{1}{2}} = y_n$$

$$x_{n+1} = x_{n+\frac{1}{2}}$$

$$y_{n+1} = y_{n+\frac{1}{2}} + \frac{1}{2} T \sin\left(2\pi x_{n+\frac{1}{2}}\right)$$

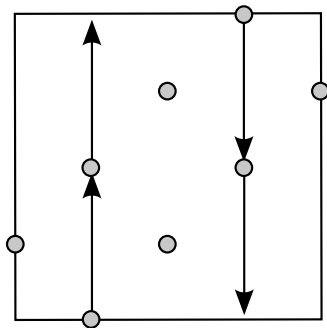
Exhibits wide range of behaviour as  $T$  is varied, from integrability to near-total chaos.

# Periodic Orbits for $T = 1$



$$\left\{ \left( \frac{1}{2}, \frac{3}{4} \right), \left( 1, \frac{3}{4} \right) \right\}$$

$$\left\{ \left( 0, \frac{1}{4} \right), \left( \frac{1}{2}, \frac{1}{4} \right) \right\}$$

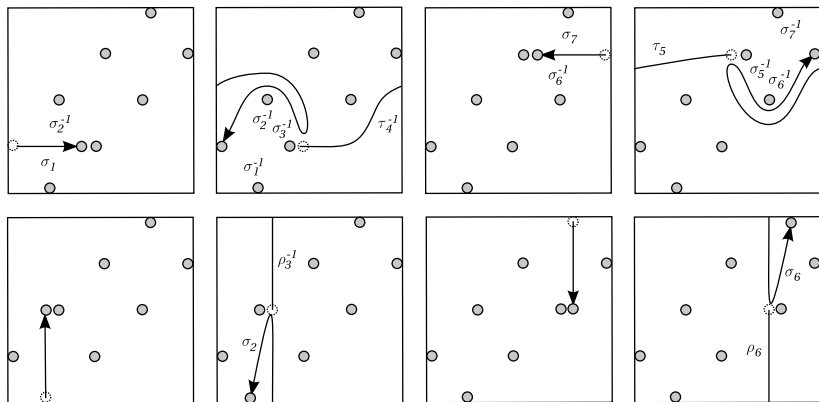


$$\left\{ \left( \frac{1}{4}, 0 \right), \left( \frac{1}{4}, \frac{1}{2} \right) \right\}$$

$$\left\{ \left( \frac{3}{4}, \frac{1}{2} \right), \left( \frac{3}{4}, 1 \right) \right\}$$

## Mapping to Braid Generators

Encode the trajectories in terms of braid group generators.

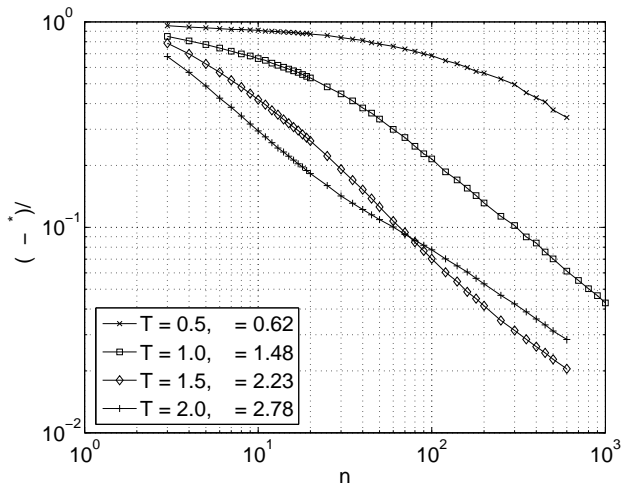


The braid word is

$\sigma_1 \sigma_2^{-1} \tau_4^{-1} \sigma_3^{-1} \sigma_2^{-1} \sigma_1^{-1} \sigma_7 \sigma_6^{-1} \tau_5 \sigma_5^{-1} \sigma_6^{-1} \sigma_7^{-1} \rho_3^{-1} \sigma_2 \rho_6 \sigma_6$ , with entropy 1.21875572687... (82% of the flow entropy).

## Convergence to Flow Entropy

Now follow arbitrary trajectories [Gambaudo (1999), Thiffeault (2005)]: the resulting nonperiodic braid has entropy that converges to the 'true' entropy of the flow.





# Conclusions

- Compute topological entropy of braids.
- Unlike train-tracks, not exact, but very accurate for braids with a pA component.
- Exact entropies by 'short-circuiting.'
- Fast! Use integer arithmetic or double precision.
- Allows the use of extremely long 'random braids' with millions of generators.
- An easy way to estimate the topological entropy of a flow. Even accessible experimentally!
- See <http://arXiv.org/nlin/0603003> for preprint.

# References



M. BESTVINA AND M. HANDEL, *Train-tracks for surface homeomorphisms*, *Topology*, 34 (1995), pp. 109–140.



J. S. BIRMAN, *On braid groups*, *Comm. Pure Appl. Math.*, 22 (1969), pp. 41–72.



P. L. BOYLAND, *Topological methods in surface dynamics*, *Topology Appl.*, 58 (1994), pp. 223–298.



P. L. BOYLAND, H. AREF, AND M. A. STREMLER, *Topological fluid mechanics of stirring*, *J. Fluid Mech.*, 403 (2000), pp. 277–304.



I. A. DYNNIKOV, *On a Yang–Baxter map and the Dehornoy ordering*, *Russian Math. Surveys*, 57 (2002), pp. 592–594.



M. D. FINN, J.-L. THIFFEAULT, AND E. GOUILLART, *Topological chaos in spatially periodic mixers*, *Physica D*, (2006), arXiv:nlin/0507023.  
in press.



J.-M. GAMBAUDO AND E. E. PÉCOU, *Dynamical cocycles with values in the Artin braid group*, *Ergod. Th. Dynam. Sys.*, 19 (1999), pp. 627–641.



T. HALL, *Train: A C++ program for computing train tracks of surface homeomorphisms*.  
[http://www.liv.ac.uk/maths/PURE/MIN\\_SET/CONTENT/members/T\\_Hall.html](http://www.liv.ac.uk/maths/PURE/MIN_SET/CONTENT/members/T_Hall.html).



B. KOLEV, *Entropie topologique et représentation de Burau*, *C. R. Acad. Sci. Sér. I*, 309 (1989), pp. 835–838.  
English translation available at <http://arxiv.org/abs/math.DS/0304105>.



J.-O. MOUSSAFIR, *On the entropy of braids*.  
In submission, 2006, arXiv:math.DS/0603355.



J.-L. THIFFEAULT, *Measuring topological chaos*, *Phys. Rev. Lett.*, 94 (2005), p. 084502.